1-D Convolutional Graph Convolutional Networks for Fault Detection in Distributed Energy Systems

Bang L.H. Nguyen[†§], Tuyen Vu[†], Thai-Thanh Nguyen[‡], Mayank Panwar[§], Rob Hovsapian[§],
[†]*ECE Department, Clarkson University*, Potsdam, NY, USA
[‡]*New York Power Authority*, White Plains, NY, USA
[§]*National Renewable Energy Research Laboratory*, Golden, CO, USA
bang.nguyen@nrel.gov, tvu@clarkson.edu, thaithanh.nguyen@nypa.gov,
mayank.panwar@nrel.gov, rob.hovsapian@nrel.gov

2022 IEEE 1st Industrial Electronics Society Annual On-Line Conference (ONCON) | 979-8-3503-9806-9/22/$31.00 ©2022 IEEE | DOI: 10.1109/ONCON56984.2022.10126859

***Abstract*— This paper presents a 1-D convolutional and graph convolutional networks for fault detection in microgrids. The combination of 1-D convolutional neural networks (1D-CNN) and graph convolutional networks (GCN) helps extract both spatial-temporal correlations from the voltage measurements in microgrids. The fault detection scheme includes fault event detection, fault type and phase classification, and fault location. There are five neural network model training to handle these tasks. Transfer learning and fine-tuning are applied to reduce training efforts. The combined 1-D convolutional and graph convolutional networks (1D-CGCN) is compared with the traditional ANN structure on the Potsdam 13-bus microgrid dataset. The accuracy of 99.5%, 98.4%, 99.2%, and 95.5% are achieved in fault event detection, fault type classification, fault phase identification, and fault location respectively. The detailed confusion matrices of fault type and fault phase classification are provided for validation.**

***Keywords*— Fault detection, fault location, microgrid protection, deep neural network, graph learning.**

I. INTRODUCTION

Fault diagnostic plays a key role to determine the strategy of how to isolate and restore power systems, especially under the growing integration of distributed energy resources. The protection and restoration strategy ensures the system's resiliency and reliability [1], [2]. In inverter-based distributed energy resources, the traditional relay protection may become ineffective due to the small fault current [3], [4], [5]. Moreover, to effectively and accurately isolate faults and restore normal operation, one requires the information of fault event, fault type, fault phase, and fault location [6], [7]. The correct information about faults significantly enhances the protection and restoration and also saves time and cost of utilities [8], [9], [10].

The fault diagnostic schemes existing in literature [11]–[24] can be loosely divided into model-based and data-driven methods. The measurements are voltage and current with different sampling rates from digital relays, phasor measurement units (PMU), or advance metering infrastructure (AMI) [25]. Model-based techniques try to compute quantitative metrics that distinguish fault data from normal measurements. A comparison between pre-fault data and fault data is usually evaluated for fault detection [26], [27]. There are many analytical approaches are applied such as evaluating the negative and positive sequences of current [26], assessing the sequential voltage and current components [28], monitoring the transient of current [27], computing the Teager-Kaiser energy [29], analyzing the principal components and fault signatures [30], and state estimation using mathematical morphology and recursive least square [31].

Data-driven and machine learning-based approaches try to derive a fault detection model using statistical information from the measurement data. There are many popular machine learning classifiers have been applied to detect faults such as decision tree (DT) [4], random forest (RF) [32], k-nearest neighbor (k-NN), support vector machine (SVM), and Naïve Bayes [33]. Model-based and machine learning can be combined in the way that model-based techniques do the feature extraction and machine learning do the classification. In [10], discrete wavelet transform is applied before the classification process. The maximal overlap discrete wavelet transform and extreme gradient boost algorithm are employed in [34]. Pure neural network structures are employed frequently such as Taguchi-based artificial neural networks [35], and gated-recurrent-unit deep neural networks [36].

Most existing works analyze the current measurements on the line the fault occurs. There is some fault detection scheme using PMU and pseudo-measurements [37], [38], [39]. Similarly, the machine learning techniques of SVM, k-NN, DT algorithms [39], convolutional neural networks (CNN) [40], [41], semi-supervised [42], and GCN [43] are implemented to detect faults. However, in these works, there is a research gap in fault type, fault phase classification, and fault location on mesh-topology power distribution systems.

This paper presents a combination of 1-D convolutional neural networks and graph neural networks on voltage measurement data to detect fault events, to classify fault type and phase, and to locate the nearest bus where the fault occurs. The paper provides a unique contribution owing to the following bullet points.

- The data input includes voltage measurements in time series from PMU, AMI, or smart meters. The

time synchronization for phasors is not necessary.

- The combination of 1-D CNN and GCN can extract both spatial and temporal correlation in the measurement data.
- The fault event detection, fault type, phase classification, and fault location are all resolved.

The remaining parts are organized as follows. Section II presents the Potsdam microgrids and the graph data collection procedure. In Section III, the combination of 1-D CNN and GCN is described. The training, transfer learning, and fine-tuning processes are also expressed. The results are discussed in Section IV. Section V concludes the paper.

II. Graph Dataset of Potsdam Microgrid

The power distribution networks can be defined as an undirected graph $\mathcal{G} = (\mathcal{V}, \mathcal{E}, \mathcal{A})$, where $\mathcal{V}$ denotes the set of vertices, $|\mathcal{V}| = N$, each vertex in the graph represents a node (bus) in the distribution network, $X = \{X_1, X_2, \dots X_N\}$ is the tuple of node features, $\mathcal{E}$ denotes the set of edges, $|\mathcal{E}| = M$, each edge represents a branch connecting two buses, $E = \{E_1, E_2, \dots E_M\}$ is the tuple of edge feature, and $\mathcal{A} \in \mathbb{R}^{N\times N}$ denotes the adjacency matrix of the distribution network. The input data for graph learning are the node features $X_{i=1\dots N}$, and the edge features $E_{i=1\dots M}$. Some papers also consider the edge features and the attributes for each graph data (u) [44]; however, in this paper, we only consider the node features on a graph.

The temporal graph dataset is constructed by the ordered set of graph, node feature matrix, and label vector tuples [45] $\mathcal{D} = \{(\mathcal{G}^1, X^1, y^1), (\mathcal{G}^2, X^2, y^2), \dots (\mathcal{G}^I, X^I, y^I)\}$, where the vertex sets is unchanged $\mathcal{V}^i = \mathcal{V}, \forall i \in \{1, \dots, I\}$, i is the graph data index. The node feature matrices $X^i \in \mathbb{R}^{N\times d\times K}$ have 3 dimensions as follows: the number of nodes $|\mathcal{V}| = N$, the number of features in each node d, and the time interval K. The label vector includes 3 labels of the distribution network graph over the time interval K, $y^i = \{y_{type}, y_{phase}, y_{loc}\}$, where y_{loc} is the node index where the fault occurs.

The node feature matrix $X^i = \{X_1, X_2, \dots X_N\}$ contains the bus voltages of all measured buses. In the bus without voltage measured, the node features are filled with zeros. The node feature in node i is shown in the form of

$$X_i = \begin{bmatrix} V_{a,1} & V_{a,2} & \cdots & V_{a,K} \\ V_{b,1} & V_{b,2} & \cdots & V_{b,K} \\ V_{c,1} & V_{c,2} & \cdots & V_{c,K} \end{bmatrix}^T, \quad (1)$$

where K is the length of the evaluation period.

Specifically, considering the Potsdam microgrid shown in Fig. 1, we have a graph of 13 nodes and 13 edges. There are 5 inverter-based generators (IBG) with a primary r

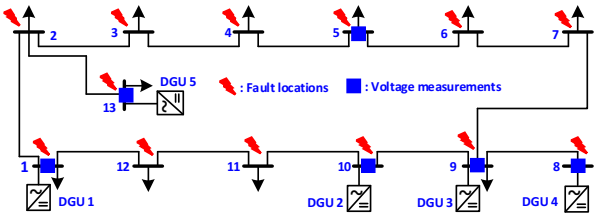

Fig. 1. 13-bus Potsdam microgrid system diagram with fault locations and voltage measurements on buses 1, 5, 8, 9, 10, and 13.

TABLE I. Potsdam Microgrid Dataset

Parameters	Configuration	Count
Fault type	AG, BG, CG, AB, BC, CA, ABG, BCG, CAG, ABC, ABCG	11
Fault resistance	0.1, 1, 10 (Ω)	3
Fault location	**Buses**: 1, 2, 3, 4, 5, 6, 7, 8, 9, 10, 11, 12, 13.	13
Load scenario	randomly	150
Total fault cases: 64,350 | **Train:** 55,770 | **Test:** 8,580		
Total load change cases: 10, 000 | **Train:** 8,580 | **Test:** 1,420		
Train-set: 64,350 samples | **Test-set**: 10,000 samples		

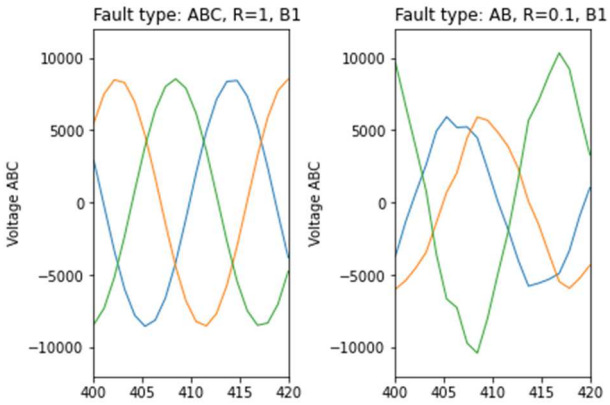

Fig. 2. Voltage waveform in phases A, B, C at bus 1 with ABC and AB faults and fault resistance 1 and 0.1 Ω occurs at bus 1, respectively, in the Potsdam microgrid.

droop control strategy [46] and a secondary PI controllefor frequency and average voltage regulation [47] in the islanded mode. The voltage level is 13.2 kV line-line at 60 Hz. The loads and IBGS have parameters following those of [48]. The voltage measurements are placed in the buses marked with a blue square; the data sampling frequency is 1 kHz. The data is collected via real-time simulation using Opal-RT.

Load changes are set randomly between 30-130% of the nominal load profile. Faults are set at each bus in turn with the fault type of AG, BG, CG, AB, BC, CA, ABG, BCG, CAG, ABC, and ABCG and fault resistance of 0.1, 1, and 10 Ω. The raw data are collected as one second windows and then are trimmed into 20 ms of 20 samples which cover about 1.2 cycles of 60 Hz as shown in Fig. 2. Thereafter, 55,770 graph data of 20-ms windows for the

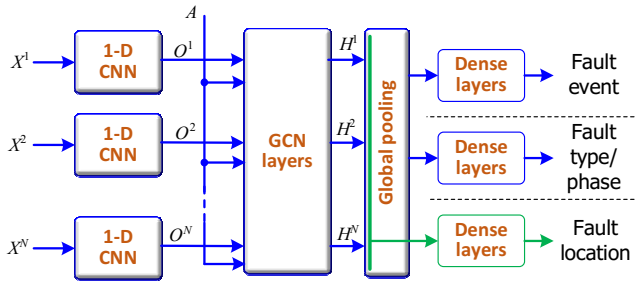

Fig. 3. Proposed temporal 1D-CGCN structure for fault detection.

fault cases and 8,580 graph data of non-fault cases with random load changes are gathered as the train set. We also select 8,580 fault and 1,420 non-fault cases for the test set. Table I summarizes these configurations for fault cases and load changes data generation.

III. 1-D Convolutional Graph Convolutional Networks Models for Fault Detection.

The proposed temporal 1D-CGCN structure for fault detection is depicted in Fig. 3. We utilize the 1-D CNN to extract the temporal correlation in time series data of voltage measurement in each bus. Thereafter, the GCN layers are used to generalize the spatial correlation on graph of the Potsdam microgrid. This combination considers the spatial-temporal correlation in the measurement data. The global pooling operation concentrates all hidden features from nodes and finally, the dense layers are trained to classify the fault type and fault phase. The fault location is performed based on all hidden features from all the nodes without using the pooling operation. The formulation of 1-D CNN and GCN layers is presented as follows.

1-D Convolutional Neural Network:

The 1D CNN layer [49] is expressed as

$$o_k^l = \sigma\left[\sum_{i=1}^{N_{l-1}} Conv1D\left(\omega_{ik}^{l-1}, o_i^{l-1}\right) + b_k^l\right], \quad (2)$$

where o_i^{l-1} is the input of 1-D CNN layer l, $o_i^0 = X_i$ is the input feature, o_i^l is the output of 1-D CNN layer l, ω_{ik}^{l-1} are the trainable weights at layer l, b_k^l is the biases of 1-D CNN layer l, $Conv1D$ is the valid cross-correlation operator, $\sigma(\cdot)$ is the activation function.

Graph Convolutional Network:

The node feature at each time index is processed by the GCN layers [50], which can be expressed as

$$H_{(l+1)}^i = \sigma\left(\tilde{D}^{-\frac{1}{2}}\tilde{A}\tilde{D}^{-\frac{1}{2}}H_{(l)}^i W_{(l)}\right), \quad (3)$$

where $\tilde{A} = A + I_N$ is the adjacent matrix with self-connection, I_N is the identity matrix, $\tilde{D}$ is the agree matrix from $\tilde{A}$ with $\tilde{D}_{ii} = \sum_i \tilde{A}_{ij}$ and $\tilde{D}_{ij} = 0$, $H_{(l+1)}^i$ is the output of GCN layer l, $H_{(l)}^i$ is the input of GCN layer l, $H_{(0)}^i = O^i$, $W_{(l)}$ is the weight matrix of layer l, $\sigma(\cdot)$ is a nonlinear activation function. This graph propagation formula can be derived as a first-order approximation of localized spectral filers [44].

TABLE II. Comparisons of Neural Network Structures

ANN		1D-CGCN	
Shared feature extraction layers			
Input	[780]	Input	[13×3×20]
Dense	[512]	1D-CNN	[13×3×5]
Dense	[128]	GCN	[13×8]
Fault event binary classification – Dense layers			
Dense	[32]	Dense	[16]
Dense	[1]	Dense	[1]
Fault location – Dense layers			
Dense	[64]	Dense	[13×8]
Dense	[13]	Dense	[13]
Fault type classification– Dense layers			
Dense	[64]	Dense	[32]
Dense	[6]	Dense	[6]
Fault phase classification– Dense layers			
Dense	[64]	Dense	[32]
Dense	[3]	Dense	[3]

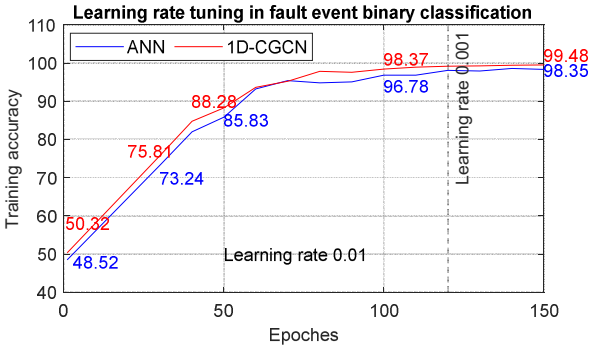

Fig. 4. The training accuracy curves with ANN and 1D-CGCN structures under the change of learning rate from 0.01 to 0.001 at epoch 120.

The detail structures of ANN and 1D-CGCN are compared in Table II, where we have shared layers for feature extraction and dense layers for classification models (classifiers). Reshaping and flattening operations are applied appropriately to condition the dimension compatibility between layers. There are 4 classifiers for fault event detection, fault location, fault type classification, and fault phase identification.

The outputs of fault event detection are fault and no-fault. The fault types are classified into six types included **1)** no-fault (**NF**), **2)** single-phase-to-ground (**LG**), **3)** two-phase (**LL**), **4)** two-phase-to-ground (**LLG**), **5)** three-phase (**3L**), and **6)** three-phase-to-ground (**3LG**). Therefore, $y_{type} \in \mathbb{B}^{1\times 6}$ with the i-th element of y_{type}: $y_{type}[i] = 1$ indicates the i-th fault category occurred

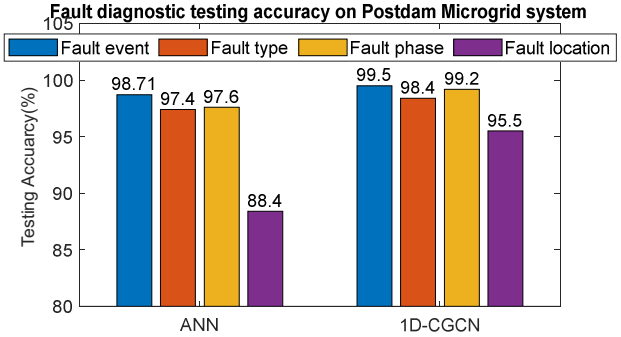

Fig. 5. Fault detection accuracy of Potsdam Microgrid system using proposed 1D-CGCN in comparison with ANN structure.

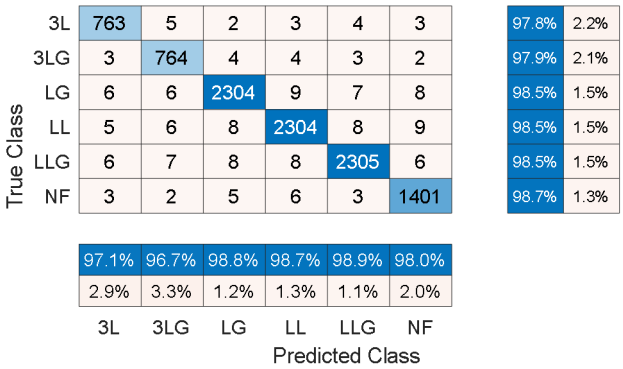

Fig. 6. Confusion matrix for fault type classification using 1D-CGCN of Potsdam microgrid test set.

while all other $y_{type}[i] = 0$. The fault phases are determined by $y_{phase} \in \mathbb{B}^{1\times 3}$, where $y_{phase}[i] = 1$ indicating the fault occurs in phase A, B, C, or AB, BC, CA when the fault types are asymmetrical i.e. LG, LL, and LLG, respectively. The fault location is indicated by $y_i = 1$, where $i = 1, 2, 3, \ldots N$ if the fault occurs in the i-th bus, otherwise $y_i = 0$. The fault location detection is performed at node-level classification, where the faulty bus is labeled as 1 and the non-fault bus is labeled as 0.

The graph dataset is trained with Adam optimizer and cross-entropy losses. The random dropout of 10% is added in dense layers to reduce overfitting. The learning rate is started at 0.01 and then is reduced to 0.001 at epoch 120 as shown in Fig. 4. The training accuracies become saturated with the learning rate of 0.01 after 120 epochs. As can be seen, the training accuracies of ANN and 1D-CGCN achieve 98.35% and 99.48%, respectively after reducing the learning rate to 0.001.

After training the fault event classification 120 epochs, the shared feature extraction layers are transferred into 3 other models: fault type classifer, fault phase classifier and fault location. Specific dense layers are added to train again for fault type, fault phase classification, and phase location. However, the fault phase classification is only trained with unbalanced faults data. Firstly, transfer learning is performed since we freeze the transferred layers and only do training for the additional dense layers. After 120 epochs, we unfroze those transferred layers and

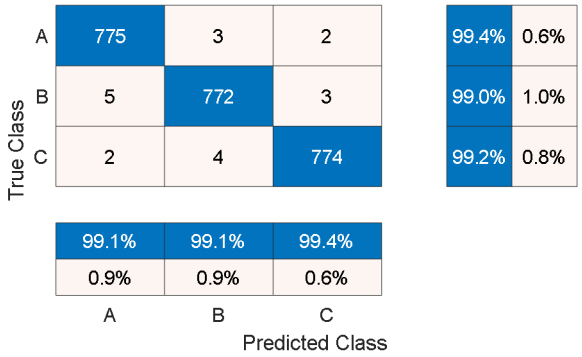

Fig. 7. Confusion matrix for fault phase A, B, and C classification using 1D-CGCN of Potsdam microgrid test set.

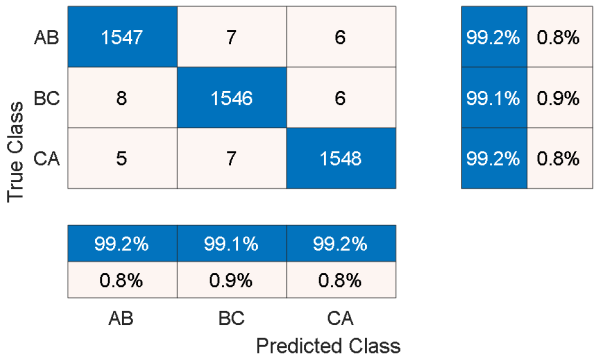

Fig. 8. Confusion matrix for fault phase AB, BC, and CA classification using 1D-CGCN of Potsdam microgrid test set.

train again the entire models with 0.001 learning rate for the fine-tuning process.

IV. Results and Discussion

The training and test results are collected on a personal computer with Intel Core i7-8700, 32 GHz, 32 GB RAM, and NVIDIA GTX 1080 GPU. The machine learning framework is Pytorch with Pytorch-geometric library for graph learning [51].

The fault detection accuracies of ANN and the proposed 1D-CGCN are compared in Fig. 5. As can be seen, for the fault event detection, ANN achieves 98.71% while 1D-CGCN can achieve 99.5%. For the fault type classification, 1D-CGCN have 1% higher than ANN since the two structures achieve 97.4% and 98.4% respectively. The 1D-CGCN is outperformed in fault phase identification with 99.2% compared to 97.6% of the ANN. Similarly, the 95.5% accuracy with 1D-CGCN in fault location compared to only 88.4% of ANN.

The detailed confusion matrix of fault type classification is shown in Fig. 6. There are 780 samples for each 3L and 3LG faults, 2340 samples for each LG, LL and LLG faults, and 1420 samples for non-fault in the total of 10,000 samples of the test set. As can be seen, the 3L and 3LG faults have less accuracy compared to other fault types.

The detailed confusion matrices of fault phase identification are shown in Figs. 7 and 8. There are 780 graph data for each phase (AG, BG, CG) in the total 2340

line-ground (LG) fault. There are 1560 graph data for each cases of AB/ABG, BC/BCG, and CA/CAG in the total of 2340 line-line (LL) fault and 2340 double line-ground (LLG) fault. The values in those confusion matrices are consistent with the testing accuracy in Fig. 5. Those results prove the high performance of the proposed fault detection models using 1D-CGCN.

V. Conclusion

In this paper, we propose a combination of 1D-CNN and GCN named 1D-CGCN for fault detection in distributed energy systems. The voltage measurements are inputs of the fault detection models. The detection models handle fault event detection, fault type and phase classification, and fault location. The real-time simulation graph data from the Potsdam microgrid using Opal-RT are collected and trained for the models. Transfer learning and fine-tuning techniques are applied to reduce training efforts. The performance of 1D-CGCN is compared with the traditional ANN to prove its superiority. The detailed confusion matrices of the classification tasks are shown for validation.The high accuracies are achieved with proposed 1D-CGCN classification models.

Although the proposed 1D-CGCN can achieve high accuracies, however, the effects of measurement noises and the lack of measurement data are not considered. Those issues would be tackled in future work.

Acknowledgment

The information, data, or work presented herein was funded in part by the 1) U.S. Office of Naval Research under award number N000142212239, and 2) National Science Foundation (NSF-AMPS) under award number CON0002619.

We also want to acknowledge Ha Ngo and Shuvangkar Das for helpful discussion on the data collection procedure and deep graph learning.

References

[1] A. Bahmanyar, S. Jamali, A. Estebsari, and E. Bompard, "A comparison framework for distribution system outage and fault location methods," *Electr. Power Syst. Res.*, vol. 145, pp. 19–34, Apr. 2017.

[2] A. Zidan *et al.*, "Fault Detection, Isolation, and Service Restoration in Distribution Systems: State-of-the-Art and Future Trends," *IEEE Trans. Smart Grid*, vol. 8, no. 5, pp. 2170–2185, Sep. 2017.

[3] M. Khederzadeh and A. Beiranvand, "Identification and Prevention of Cascading Failures in Autonomous Microgrid," *IEEE Syst. J.*, vol. 12, no. 1, pp. 308–315, Mar. 2018.

[4] D. P. Mishra, S. R. Samantaray, and G. Joos, "A combined wavelet and data-mining based intelligent protection scheme for microgrid," *IEEE Trans. Smart Grid*, vol. 7, no. 5, pp. 2295–2304, 2016.

[5] A. Hooshyar, E. F. El-Saadany, and M. Sanaye-Pasand, "Fault Type Classification in Microgrids Including Photovoltaic DGs," *IEEE Trans. Smart Grid*, vol. 7, no. 5, pp. 2218–2229, Sep. 2016.

[6] M. A. Azzouz, A. Hooshyar, and E. F. El-Saadany, "Resilience Enhancement of Microgrids With Inverter-Interfaced DGs by Enabling Faulty Phase Selection," *IEEE Trans. Smart Grid*, vol. 9, no. 6, pp. 6578–6589, Nov. 2018.

[7] T. Fahey and N. Burbure, "Single-Phase Tripping," *IEEE Power Energy Mag.*, vol. 6, no. 2, pp. 46–52, Mar. 2008.

[8] J. R. Aguero, J. Wang, and J. J. Burke, "Improving the reliability of power distribution systems through single-phase tripping," in *IEEE PES T&D 2010*, 2010, pp. 1–7.

[9] R. M. Cheney, J. T. Thorne, and G. Hataway, "Distribution single-phase tripping and reclosing: Overcoming obstacles with programmable recloser controls," in *2009 Power Systems Conference*, 2009, pp. 1–10.

[10] A. Borghetti, M. Bosetti, C. A. Nucci, M. Paolone, and A. Abur, "Integrated Use of Time-Frequency Wavelet Decompositions for Fault Location in Distribution Networks: Theory and Experimental Validation," *IEEE Trans. Power Deliv.*, vol. 25, no. 4, pp. 3139–3146, Oct. 2010.

[11] A. M. Tsimtsios and V. C. Nikolaidis, "Towards Plug-and-Play Protection for Meshed Distribution Systems With DG," *IEEE Trans. Smart Grid*, vol. 11, no. 3, pp. 1980–1995, May 2020.

[12] W. T. El-Sayed, M. A. Azzouz, H. H. Zeineldin, and E. F. El-Saadany, "A Harmonic Time-Current-Voltage Directional Relay for Optimal Protection Coordination of Inverter-Based Islanded Microgrids," *IEEE Trans. Smart Grid*, vol. 12, no. 3, pp. 1904–1917, May 2021.

[13] M. Shafiei, F. Golestaneh, G. Ledwich, G. Nourbakhsh, H. B. Gooi, and A. Arefi, "Fault Detection for Low-Voltage Residential Distribution Systems With Low-Frequency Measured Data," *IEEE Syst. J.*, vol. 14, no. 4, pp. 5265–5273, Dec. 2020.

[14] H. Jiang, J. J. Zhang, W. Gao, and Z. Wu, "Fault Detection, Identification, and Location in Smart Grid Based on Data-Driven Computational Methods," *IEEE Trans. Smart Grid*, vol. 5, no. 6, pp. 2947–2956, Nov. 2014.

[15] T. Wu, Y.-J. Angela Zhang, and X. Tang, "Online Detection of Events With Low-Quality Synchrophasor Measurements Based on iForest," *IEEE Trans. Ind. Informatics*, vol. 17, no. 1, pp. 168–178, Jan. 2021.

[16] H. Hassani, R. Razavi-Far, and M. Saif, "Fault Location in Smart Grids Through Multicriteria Analysis of Group Decision Support Systems," *IEEE Trans. Ind. Informatics*, vol. 16, no. 12, pp. 7318–7327, Dec. 2020.

[17] M. A. Azzouz, H. H. Zeineldin, and E. F. El-Saadany, "Selective Phase Tripping for Microgrids Powered by Synchronverter-Interfaced Renewable Energy Sources," *IEEE Trans. Power Deliv.*, vol. 36, no. 6, pp. 3506–3518, Dec. 2021.

[18] B. Wang, J. Geng, and X. Dong, "High-Impedance Fault Detection Based on Nonlinear Voltage–Current Characteristic Profile Identification," *IEEE Trans. Smart Grid*, vol. 9, no. 4, pp. 3783–3791, Jul. 2018.

[19] L. Song, X. Han, M. Yang, W. Sima, and L. Li, "Fault detection and protection in a meshed MMC HVDC grid based on bus-voltage change rate and fault component current," *Electr. Power Syst. Res.*, vol. 201, p. 107530, Dec. 2021.

[20] N. Sapountzoglou, J. Lago, B. De Schutter, and B. Raison, "A generalizable and sensor-independent deep learning method for fault detection and location in low-voltage distribution grids," *Appl. Energy*, vol. 276, p. 115299, Oct. 2020.

[21] O. F. Eikeland, I. S. Holmstrand, S. Bakkejord, M. Chiesa, and F. M. Bianchi, "Detecting and Interpreting Faults in Vulnerable Power Grids With Machine Learning," *IEEE Access*, vol. 9, pp. 150686–150699, 2021.

[22] P. Stefanidou-Voziki, D. Cardoner-Valbuena, R. Villafafila-Robles, and J. L. Dominguez-Garcia, "Data analysis and management for optimal application of an advanced ML-based fault location algorithm for low voltage grids," *Int. J. Electr. Power Energy Syst.*, vol. 142, p. 108303, Nov. 2022.

[23] S. Chakraborty and S. Das, "Application of Smart Meters in High Impedance Fault Detection on Distribution Systems," *IEEE Trans. Smart Grid*, vol. 10, no. 3, pp. 3465–3473, May 2019.

[24] M. Gilanifar *et al.*, "Multi-Task Logistic Low-Ranked Dirty Model for Fault Detection in Power Distribution System," *IEEE Trans. Smart Grid*, vol. 11, no. 1, pp. 786–796, Jan. 2020.

[25] K. Chen, C. Huang, and J. He, "Fault detection, classification and location for transmission lines and distribution systems: a review on the methods," *High Volt.*, vol. 1, no. 1, pp. 25–33, Apr. 2016.

[26] H. Muda and P. Jena, "Superimposed Adaptive Sequence Current

Based Microgrid Protection: A New Technique," *IEEE Trans. Power Deliv.*, vol. 32, no. 2, pp. 757–767, Apr. 2017.
[27] I. Sadeghkhani, M. E. Hamedani Golshan, A. Mehrizi-Sani, J. M. Guerrero, and A. Ketabi, "Transient Monitoring Function-Based Fault Detection for Inverter-Interfaced Microgrids," *IEEE Trans. Smart Grid*, pp. 1–1, 2016.
[28] A. Rahmati and R. Adhami, "A Fault Detection and Classification Technique Based on Sequential Components," *IEEE Trans. Ind. Appl.*, vol. 50, no. 6, pp. 4202–4209, Nov. 2014.
[29] M. A. Jarrahi, H. Samet, and T. Ghanbari, "Novel Change Detection and Fault Classification Scheme for AC Microgrids," *IEEE Syst. J.*, vol. 14, no. 3, pp. 3987–3998, Sep. 2020.
[30] Q. H. Alsafasfeh, I. Abdel-Qader, and A. M. Harb, "Fault Classification and Localization in Power Systems Using Fault Signatures and Principal Components Analysis," *Energy Power Eng.*, vol. 04, no. 06, pp. 506–522, 2012.
[31] T. Gush *et al.*, "Fault detection and location in a microgrid using mathematical morphology and recursive least square methods," *Int. J. Electr. Power Energy Syst.*, vol. 102, pp. 324–331, Nov. 2018.
[32] E. Casagrande, W. L. Woon, H. H. Zeineldin, and D. Svetinovic, "A Differential Sequence Component Protection Scheme for Microgrids With Inverter-Based Distributed Generators," *IEEE Trans. Smart Grid*, vol. 5, no. 1, pp. 29–37, Jan. 2014.
[33] T. S. Abdelgayed, W. G. Morsi, and T. S. Sidhu, "A New Approach for Fault Classification in Microgrids Using Optimal Wavelet Functions Matching Pursuit," *IEEE Trans. Smart Grid*, vol. 9, no. 5, pp. 4838–4846, Sep. 2018.
[34] B. Patnaik, M. Mishra, R. C. Bansal, and R. K. Jena, "MODWT-XGBoost based smart energy solution for fault detection and classification in a smart microgrid," *Appl. Energy*, vol. 285, p. 116457, Mar. 2021.
[35] Y.-Y. Hong and M. T. A. M. Cabatac, "Fault Detection, Classification, and Location by Static Switch in Microgrids Using Wavelet Transform and Taguchi-Based Artificial Neural Network," *IEEE Syst. J.*, vol. 14, no. 2, pp. 2725–2735, Jun. 2020.
[36] J. J. Q. Yu, Y. Hou, A. Y. S. Lam, and V. O. K. Li, "Intelligent Fault Detection Scheme for Microgrids With Wavelet-Based Deep Neural Networks," *IEEE Trans. Smart Grid*, vol. 10, no. 2, pp. 1694–1703, Mar. 2019.
[37] M. Farajollahi, A. Shahsavari, E. M. Stewart, and H. Mohsenian-Rad, "Locating the Source of Events in Power Distribution Systems Using Micro-PMU Data," *IEEE Trans. Power Syst.*, vol. 33, no. 6, pp. 6343–6354, Nov. 2018.
[38] Y. Zhang, J. Wang, and M. E. Khodayar, "Graph-Based Faulted Line Identification Using Micro-PMU Data in Distribution Systems," *IEEE Trans. Smart Grid*, vol. 11, no. 5, pp. 3982–3992, Sep. 2020.
[39] A. Shahsavari, M. Farajollahi, E. M. Stewart, E. Cortez, and H. Mohsenian-Rad, "Situational Awareness in Distribution Grid Using Micro-PMU Data: A Machine Learning Approach," *IEEE Trans. Smart Grid*, vol. 10, no. 6, pp. 6167–6177, Nov. 2019.
[40] W. Li, D. Deka, M. Chertkov, and M. Wang, "Real-time Faulted Line Localization and PMU Placement in Power Systems through Convolutional Neural Networks," *IEEE Trans. Power Syst.*, vol. 34, no. 6, pp. 4640–4651, 2018.
[41] K. Chen, J. Hu, Y. Zhang, Z. Yu, and J. He, "Fault Location in Power Distribution Systems via Deep Graph Convolutional Networks," *IEEE J. Sel. Areas Commun.*, vol. 38, no. 1, pp. 119–131, Jan. 2020.
[42] Q. Cui and Y. Weng, "Enhance High Impedance Fault Detection and Location Accuracy via μ -PMUs," *IEEE Trans. Smart Grid*, vol. 11, no. 1, pp. 797–809, Jan. 2020.
[43] L. Wenlong, Y. Dechang, W. Yusen, and R. Xiang, "Fault diagnosis of power transformers using graph convolutional network," *CSEE J. Power Energy Syst.*, 2020.
[44] P. W. Battaglia *et al.*, "Relational inductive biases, deep learning, and graph networks," Jun. 2018.
[45] B. Rozemberczki *et al.*, "PyTorch Geometric Temporal: Spatiotemporal Signal Processing with Neural Machine Learning Models," Apr. 2021.
[46] D. E. Olivares *et al.*, "Trends in microgrid control," *IEEE Trans. Smart Grid*, vol. 5, no. 4, pp. 1905–1919, 2014.
[47] B. L. H. Nguyen, T. V. Vu, T. H. Ortmeyer, and T. Ngo, "Distributed Dynamic State Estimation for Microgrids," in *2020 IEEE Power & Energy Society General Meeting (PESGM)*, 2020, pp. 1–5.
[48] B. L. H. Nguyen, T. V. Vu, J. M. Guerrero, M. Steurer, K. Schoder, and T. Ngo, "Distributed dynamic state-input estimation for power networks of Microgrids and active distribution systems with unknown inputs," *Electr. Power Syst. Res.*, vol. 201, p. 107510, Dec. 2021.
[49] S. Kiranyaz, O. Avci, O. Abdeljaber, T. Ince, M. Gabbouj, and D. J. Inman, "1D convolutional neural networks and applications: A survey," *Mech. Syst. Signal Process.*, vol. 151, p. 107398, Apr. 2021.
[50] T. N. Kipf and M. Welling, "Semi-Supervised Classification with Graph Convolutional Networks," Sep. 2016.
[51] M. Fey and J. E. Lenssen, "Fast Graph Representation Learning with PyTorch Geometric," Mar. 2019.